

GPU Accelerated RIS-based Influence Maximization Algorithm

Soheil Shahrouz, Saber Salehkaleybar, and Matin Hashemi

Abstract—Given a social network modeled as a weighted graph G , the influence maximization problem seeks k vertices to become initially influenced, to maximize the expected number of influenced nodes under a particular diffusion model. The influence maximization problem has been proven to be NP-hard, and most proposed solutions to the problem are approximate greedy algorithms, which can guarantee a tunable approximation ratio for their results with respect to the optimal solution. The state-of-the-art algorithms are based on Reverse Influence Sampling (RIS) technique, which can offer both computational efficiency and non-trivial $(1 - 1/e - \epsilon)$ -approximation ratio guarantee for any $\epsilon > 0$. RIS-based algorithms, despite their lower computational cost compared to other methods, still require long running times to solve the problem in large-scale graphs with low values of ϵ . In this paper, we present a novel and efficient parallel implementation of a RIS-based algorithm, namely IMM, on GPGPU. The proposed solution can significantly reduce the running time on large-scale graphs with low values of ϵ . Furthermore, we show that our proposed parallel algorithm can solve other variations of the IM problem, only by applying minor modifications. Experimental results show that the proposed solution reduces the runtime by a factor up to $220\times$.

Index Terms—CUDA, GPGPU, Graph Diffusion Process, Influence Maximization (IM), Parallel Processing, Reverse Influence Sampling (RIS).

1 INTRODUCTION

WITH the explosion of social network services in the last decades, hundreds of millions of people can easily interact with each other. The vast prevalence of social networks facilitates large-scale viral marketing through “word-of-mouth” effects, where each individual recommends a product to his/her friends, contributing to a large number of adoptions of the product. In order to succeed in a viral marketing campaign, it is required to choose a few *influential* individuals and provide incentives (e.g. free samples of the product and/or cash) to create a cascade of product adoptions as large as possible. Obtaining such a set of users is commonly known as the “influence maximization (IM) problem”. In particular, for a given network G and a probability model representing diffusion mechanism in the network, IM aims to select a set of users (called seed set) which maximizes the expected number of users that are affected in the diffusion process.

In a seminal work, Kempe et al. [1] formulated the IM problem as a combinatorial optimization problem for two popular diffusion models, namely, independent cascade (IC) and linear threshold (LT). They showed that the IM problem is NP-hard in both models, and proposed a greedy framework that can obtain $(1 - \frac{1}{e} - \epsilon)$ -approximate solutions for any $\epsilon > 0$. More specifically, they considered the influence spread (the expected number of affected users) as a function of seed set. Starting from an empty set, a user with the maximum marginal gain to the influence spread is added to the seed set in an iterative manner until the desired number

of users are selected. Almost all the proposed algorithms for the IM problem followed this greedy framework. Later, it has been shown that computing the influence spread as a function of seed set is #P-hard under both IC and LT models [2], [3]. These theoretical results have motivated many researchers to design efficient estimators for the influence spread. In this regard, existing algorithms for the IM problem can be classified into three main approaches: I) simulation-based approach, II) proxy-based approach, and III) sketch-based approach.

In the simulation-based approach, Monte Carlo (MC) simulations are executed to estimate the influence spread for a given seed set by averaging the number of affected users over all the generated instances. This approach was considered in [1] for the first time and subsequent works tried to reduce the number of MC simulations through *lazy evaluation* [4], [5]. The main advantage of this approach is that it can be utilized for any diffusion model. However, it is not scalable to very large graphs since it requires to generate too many instances to compute the influence spread with a desirable estimation error. In the proxy-based approach, the main idea is to use simple models, such as shortest path or PageRank, instead of complicated diffusion models. This reduces the runtime for computing the influence spread significantly. However, improving the time complexity of evaluating the influence spread comes at the expense of losing theoretical guarantees on estimation error bounds. In fact, it has been shown that the proxy-based approach might have unstable behavior in some graphs in the sense that the influence spread could change significantly by a small modification in the graph structure [6]. The sketch-based approach has been proposed to overcome computational inefficiency issues of the simulation-based approach and instability problems of the proxy-based approach. The main

Authors are with Learning and Intelligent Systems Laboratory, Department of Electrical Engineering, Sharif University of Technology, Tehran, Iran. E-mails: soheil.shahrouz@ee.sharif.edu, saleh@sharif.edu (corresponding author), matin@sharif.edu. Webpage: <http://lis.ee.sharif.edu>

idea is to first generate *sketches* for a given diffusion model. Afterwards, the influence spread is estimated based on the generated sketches. Due to the desired properties of this approach, many recent algorithms for the IM problem have focused on efficiently generating sketches (see Section 2).

Although the most recent algorithms for the IM problem are mainly based on constructing sketches, they still have computational issues for small estimation error bounds in large graphs. Moreover, this problem might become critical in some recent applications of IM such as multi-round IM [7], where it is required to solve the IM problem multiple times for a given graph.

The aim of this paper is to accelerate the state-of-the-art sketch-based algorithm (IMM [8]) using parallel processing on GPU. Our main contributions are as follows:

- One of the key parts in IMM algorithm is to find a reverse reachable set of nodes from a randomly selected node by executing a BFS algorithm. This part of the algorithm is repeated multiple times. Many common approaches for the acceleration of BFS on GPU run only one BFS at a time, and therefore, produce a single reverse reachable set. Here, we propose a method to simultaneously generate multiple reverse reachable sets, and at the same time, parallelize each task of generating a reverse reachable set as well. More specifically, several BFSs are executed in parallel, and in each one, adjacent edges of a node are processed in parallel, but nodes in the frontier queue are processed sequentially (Section 3.2).
- We also propose methods to judiciously store large frontier queues of the BFSs in limited GPU shared memory in order to further reduce the runtime (Section 3.3).
- We propose data structures and methods to optimally store the sketches in GPU global memory (Section 3.5) and to process them efficiently in order to select the seed set (Section 3.7). This helps to fit the required internal data structures into GPU global memory for large graphs with millions of nodes.
- The proposed parallelization of IMM algorithm on GPU can be utilized in other applications that use a variant of IMM algorithm as a subroutine. For instance, we show that our implementation can be adapted to the multi-round IM problem. The experiments show that running times are greatly reduced (Section 4.5).
- Experimental results on real social networks show that the proposed parallel algorithm can outperform state-of-the-art solutions by a factor of up to $220\times$.

The rest of this paper is organized as follows: Section 2 reviews preliminaries on diffusion models, the basic greedy algorithm, and RIS-based algorithms. Section 3 presents our proposed parallel algorithm for the IM problem. Section 4 presents experiment results and comparisons with related works. Finally, Section 5 concludes the paper.

2 PRELIMINARIES

In this section, we introduce some notations and investigate two common diffusion models, namely independent cascade and linear threshold models. Then we formally define

the influence maximization problem and review Kempe’s greedy algorithm [1] and methods based on reverse influence sampling.

2.1 Notation

Directed graph $G = (V, E)$ models a social network, where V denotes the set of vertices (i.e., users) and E indicates the set of directed edges (i.e., relationships between users). For every edge $e = (u, v) \in E$, we define u as an incoming neighbor of v , and v as an outgoing neighbor of u . Also, we denote sets of **incoming** and **outgoing** neighbors of every node u , by $N_I(u)$ and $N_O(u)$, respectively. Moreover, we assume that every edge $e = (u, v) \in E$ is associated with an **influence probability** $p_{uv} \in [0, 1]$. We denote the total number of nodes and edges in G by n and m , respectively.

2.2 Diffusion Models

There is an immense amount of literature on models that capture the diffusion phenomenon’s behavior [9], [10], [11], [12], [13], [14], [15]. Among these models, independent cascade (IC) and linear threshold (LT) models have been extensively studied. In the following, we briefly describe these two models.

Independent Cascade (IC) Diffusion Model

Given a graph $G = (V, E)$, edge influence probabilities p_{uv} for every edge $e = (u, v)$, and a subset of vertices $S \subseteq V$, which is commonly called **seed set**, an instance of influence diffusion process under the IC model is generated as follows:

The influence propagates in discrete time steps. In the beginning, i.e., at time t_0 , only the nodes in the seed set S are activated, and all the other nodes remain inactive. At every time step t_{i+1} , every node u , which has been activated at time step t_i , has a chance to activate its inactive outgoing neighbors. Node u succeeds to activate an inactive outgoing neighbor v , with probability p_{uv} . When a node is activated (either initially at t_0 or by an incoming active neighbor), it remains active in the following time steps. The influence diffusion process terminates at a time step at which none of the previously activated nodes can activate a new inactive node.

Linear Threshold (LT) Diffusion Model

The LT model imposes a new restriction on edge influence probabilities, by which the sum of probabilities of incoming edges for every node u , must be less than or equal to 1. Moreover, in the LT model, every node u is associated with a threshold τ_u , which is a real value in the range $[0, 1]$. Given a seed set S , a single diffusion process instance under LT model can be described as follows:

Similar to the IC model, the influence propagates in discrete time steps. At time step t_0 , we assign a random number sampled uniformly from $[0, 1]$ to each node u , as its threshold τ_u . Furthermore, we initially activate every node $u \in S$ and leave the other nodes as inactive. At time step t_{i+1} , every node that has been previously activated remains

active, and every inactive node v becomes active when it satisfies the following condition

$$\sum_{u \in N_I(v)} p_{uv} \cdot \mathbb{1}_A(u) \geq \tau_v, \quad (1)$$

where A is the set of all activated nodes until some time step t_i , and $\mathbb{1}_A(u)$ is indicator function which is equal to one if $u \in A$. The influence diffusion process under LT model stops at a time step at which no inactive node can become active.

2.3 Problem Statement

The **influence spread** of seed set S in a single influence diffusion process instance is defined as the total number of active nodes after the termination of the diffusion process, and is denoted by $I(S)$. It should be noted that $I(S)$ is not a deterministic function of S . The influence diffusion procedure is a random process which depends on edge influence probabilities (and also node thresholds in LT model). Therefore, $I(S)$ is a random variable.

Given graph G , edge influence probabilities p_{uv} , a particular diffusion model, and a constant positive integer k , the goal of the influence maximization problem is to find seed set $S^* \subset V$ of size k , which has the maximum **expected influence spread** $\mathbf{E}[I(S)]$. The problem can also be expressed as follows:

$$S^* = \operatorname{argmax}_{S \subset V} \{ \mathbf{E}[I(S)] \mid |S| = k \}, \quad (2)$$

where S^* is the optimal seed set with size k .

2.4 Complexity of IM Problem

It has been shown [1] that the IM problem is NP-Hard under both IC and LT diffusion models. The IM problem asks for seed set S of size k , in order to maximize $\mathbf{E}[I(S)]$, and it turns out that even evaluating $\mathbf{E}[I(S)]$, which is the term to be maximized, is not a trivial task. Actually, it has been proven that determining $\mathbf{E}[I(S)]$ is #P-Hard under both LT [2] and IC [3] diffusion models. Thus, the focus in the literature has been on proposing computationally efficient approximation algorithms, which can provide solutions to the problem with a guaranteed approximation ratio in a reasonable time.

2.5 Basic Greedy Algorithm

Kempe et al. [1] proposed a greedy algorithm to solve the IM problem. This algorithm iteratively selects nodes for insertion into the seed set. As shown in Algorithm 1, the seed set S is initialized by an empty set. In every iteration, the node v whose insertion into the seed set S leads to the largest increase in $\mathbf{E}[I(S)]$ is selected. The amount of increase is called **marginal gain**. The algorithm terminates after k iterations, i.e., when the size of seed set S reaches k .

The greedy algorithm has a simple structure, but its main drawback is that it requires $\mathbf{E}[I(S \cup u)]$ to be computed in every iteration for all the remaining nodes. As mentioned before, evaluating $\mathbf{E}[I(S)]$ has been proven to be #P-Hard. To tackle this problem, Kempe et al. [1] proposed a method based on Monte Carlo (MC) simulations in order

Algorithm 1 Basic greedy algorithm for the IM problem.

Input: G, k

Output: S

- 1: $S = \emptyset$
 - 2: **for** $i = 1$ to k **do**
 - 3: $v = \operatorname{argmax}_{u \in V \setminus S} \{ \mathbf{E}[I(S \cup u)] - \mathbf{E}[I(S)] \}$
 - 4: $S = S \cup \{v\}$
 - 5: **end for**
-

to estimate the value of $\mathbf{E}[I(S \cup u)]$. In order to execute a single Monte Carlo simulation under IC diffusion model, an **instance graph** g is created from G , by removing every edge $(u, v) \in E$ by probability $1 - p_{uv}$. **Reachable set** $R(S)$ is defined as the set of all nodes that are reachable from S in the resulted graph g . Kempe et al. have shown that $\mathbf{E}[|R(S)|] = \mathbf{E}[I(S)]$, and therefore, one can estimate $\mathbf{E}[I(S)]$ by determining $\mathbf{E}[|R(S)|]$ through running a large number of Monte Carlo simulations and generating many instances of g . They also proved that by knowing the exact values of $\mathbf{E}[I(S)]$, greedy algorithms solution has an approximation ratio of $(1 - \frac{1}{e})$. However, in practice, the value of $\mathbf{E}[I(S)]$ is estimated and the true approximation ratio is $(1 - \frac{1}{e} - \epsilon)$, in which ϵ depends on both graph G and the total number of Monte Carlo simulations. In [1], they did not provide any formal analysis on the number of required MC simulations in order to achieve $(1 - \frac{1}{e} - \epsilon)$ approximation ratio and only suggested using 10,000 MC simulations. Several following works also used 10,000 as the number of MC simulations without providing any formal analysis. Later, Chen et al. [16] conducted an analysis on the total number of MC simulations and relative error ϵ . They showed that to achieve $(1 - \frac{1}{e} - \epsilon)$ approximation ratio under both IC and LT diffusion models, with a probability of $1 - \frac{1}{n}$, one needs to execute $\Theta(\epsilon^{-2} k^2 n \log(n^2 k))$ number of MC simulations. Therefore, lower values of ϵ requires larger number of MC simulations.

2.6 RIS-based Algorithms

As shown in Algorithm 1, in every iteration, the greedy algorithm evaluates the marginal gain (i.e., the improvement in expected influence spread) resulting from adding one node which is not currently in the seed set. Thus, the number of marginal gain evaluations is $O(n)$, and because there are k iterations in total, the greedy algorithm conducts $O(nk)$ marginal gain evaluations. Every marginal gain evaluation involves calculating $\mathbf{E}[|R(S)|]$, which is a computationally expensive task, as mentioned in Section 2.4. In addition, in every iteration, we are only interested in the node with the largest marginal gain, therefore, marginal gain evaluations for all the other nodes are virtually wasted and are not useful in subsequent iterations.

To address this problem, Borgs et al. [17] proposed a method called **Reverse Influence Sampling (RIS)**, by which there is no need to run many MC simulations for every remaining node in every iteration in order to evaluate the marginal gain.

In order to describe RIS-based algorithms, we need the following definitions. Given a graph G and edge influence

Algorithm 2 RIS-based algorithm for the IM problem.

Input: G, k
Output: S

- 1: $S = \emptyset, R = \emptyset$
- 2: // Step 1: estimation and sampling
- 3: Estimate θ , i.e., the required number of RR sets
- 4: Generate θ random RR sets and insert them into R
- 5: // Step 2: maximum coverage
- 6: **for** $i = 1$ to k **do**
- 7: $v = \operatorname{argmax}_{u \in V \setminus S} \sum_{RR \in R} \mathbb{1}(u \in RR)$
- 8: $S = S \cup \{v\}$
- 9: Remove all RR sets covered by v from R
- 10: **end for**

probabilities p_{uv} for every edge $e = (u, v) \in E$, one can generate an instance graph g from G , by removing every edge $e = (u, v)$ by probability $1 - p_{uv}$. Let v be a node in graph G , then **reverse reachable (RR) set** for v in g is defined as the set of all nodes in g that can reach v . An RR set is defined to be a **random RR set** if instance graph g is created from G as described before, and node v is selected randomly from the set of nodes V .

In other words, every node u that is present in an RR set generated for a particular node v , has an opportunity to activate v , if it has been activated already. Borgs et al. [17] showed that the probability by which a node u can appear in a random RR set is proportional to the expected influence spread of “that” node. Moreover, they proved that the probability by which a particular seed set S , overlaps a random RR set can be used as an unbiased estimator of expected influence spread of the seed set, as given in the following equation:

$$\mathbb{E}[I(S)] = n \times \Pr[S \cap RR \neq \emptyset]. \quad (3)$$

According to above results, Borgs et al. [17] proposed an algorithm to solve the IM problem. As illustrated in Algorithm 2, it consists of two main steps. First, given ϵ , the required number of random RR sets θ to guarantee the approximation ratio $(1 - \frac{1}{e} - \epsilon)$ is estimated, and then, a total number of θ random RR sets are generated. Second, the problem of maximum coverage on all generated random RR sets is considered. The goal of the problem is to find a set of k nodes which covers the maximum number of RR sets. The problem is known to be NP-Hard, and it has been proven that the hill-climbing greedy algorithm yields a $(1 - \frac{1}{e})$ approximate solution. After solving the maximum coverage problem, the resulting set of nodes (of size k) is returned as the solution to the IM problem [17].

Many previous works on RIS-based influence maximization algorithms have focused on providing formal analysis on the required number of random RR sets to ensure $(1 - \frac{1}{e} - \epsilon)$ -approximation guarantee [8], [18], [19]. Specifically, most studies have tried to reduce the number of required random RR sets, while preserving theoretical guarantees. Borgs et al. [17] terminated the random RR set generation procedure when the total number of traversed edges during random RR set generation exceeds a predefined threshold τ . They showed that by setting τ equal to $O(\epsilon^{-2}k(m+n)\log(n))$, a

Algorithm 3 Estimating the lower bound LB.

Input: G, k, ϵ
Output: LB

- 1: $S = \emptyset, R = \emptyset$
- 2: **for** $i = 1$ to $\log_2(n) - 1$ **do**
- 3: $x = n/2^i$
- 4: $\theta = f(n, \epsilon, k)/x$
- 5: Sample random RR sets until $|R| < \theta$
- 6: $S = \text{SeedSelection}(R, k)$
- 7: **if** $n \times F_R(S) \geq (1 + \sqrt{2}\epsilon) \times x$ **then**
- 8: $LB = n \times F_R(S)/(1 + \sqrt{2}\epsilon)$
- 9: **break**
- 10: **end if**
- 11: **end for**

$(1 - \frac{1}{e} - \epsilon)$ -approximation solution is guaranteed. The main issue with this method is the large constant factor in the equation that determines the threshold, which incurs heavy computational cost. Tang et al. [18] proposed TIM and TIM+ algorithms. They showed that θ should be greater than $\frac{\lambda}{OPT}$, where parameter λ is a constant factor determined by n, ϵ and k , and parameter OPT is the optimal solution’s expected influence spread. Later, Tang et al. proposed IMM [8], which reduces the value of λ , and as a result, the value of θ based on a martingale approach [20]. Nguyen et al. [19] proposed SSA/DSSA algorithms and reduced θ , but later, Huang et al. [21] showed that there are some issues with SSA’s analysis and it cannot preserve theoretical guarantees.

Both TIM and IMM algorithms need optimal solution’s influence spread, i.e., OPT , in order to estimate the required number of RR sets, but in reality there is no prior knowledge on the value of OPT . These two algorithms resolve this issue by providing a (preferably close) lower bound LB for the value of OPT , and therefore, a larger estimated value for θ , i.e., $\theta = \frac{\lambda}{LB} > \frac{\lambda}{OPT}$.

To obtain a reasonable lower bound for OPT , both TIM and IMM use bootstrapping estimation techniques to perform a hypothesis testing (see Algorithm 3). They first set the value of θ with an initial estimation (line 4). We refer readers to [8], [18] for more details on the function f in line 4. Next, they sample random RR sets until the total number of RR sets reaches θ (line 5). Then, they construct a seed set from the generated RR sets. The function SeedSelection in line 6 in Algorithm 3 is equivalent to some extent to lines 6 – 10 in Algorithm 2. After that, they estimate the influence spread of the generated seed set and compare it with the approximation bound of the estimator (line 7). If the estimated influence spread is much higher than the approximation bound, they use a discounted value of that estimate as LB (line 8). Otherwise, they double the number of RR sets (lines 3 – 4) and repeat the described procedure.

3 PROPOSED RIS-BASED PARALLEL ALGORITHM

In this section, we present our solution to accelerate computational bottlenecks of RIS-based algorithms on GPU using CUDA framework. Similar to IMM, our solution is composed of two main steps: 1) sampling RR sets, and 2) generating the seed set.

3.1 Baseline Parallel Methods for RR Set Sampling

Before discussing our proposed method, we first investigate two simpler approaches that can be used to parallelize random RR set generation in RIS-based algorithms. For each of these two approaches, we first explain the method and then mention its drawbacks. Our proposed parallel method for RR set sampling will be discussed in Section 3.2.

Thread-Level Parallelization:

Since in RIS-based algorithms, every random RR set can be generated independently from other random RR sets, one simple approach to parallelize random RR set generation is to assign the task of creating every random RR set to one thread, and launch a large number of threads on GPU.

The main issue with this approach is its severe workload imbalance. Since size of a random RR set may range from a single node to a large portion of the graph, and node degrees vary as well, the amount of work to generate a random RR set varies drastically. This causes severe workload imbalance among the threads within a block, which makes a large number of threads inactive most of the time, and hence, highly degrades the overall performance.

Memory capacity is another impediment to this approach. Since every thread needs to separately maintain large arrays (e.g., visited nodes), memory capacity can easily become the bottleneck and prevent this approach to scale-up to large graphs with millions of nodes.

Parallel Breadth First Search:

Generating a random RR set is equivalent to running breadth-first search (BFS) algorithm starting from a randomly selected node on a reversed instance graph. One can avoid generating a whole reversed instance graph by incorporating instance graph generation into the BFS algorithm. In the standard BFS, once a node u is picked up from the front of the frontier queue, all of its outgoing edges are traversed. If instead of traversing all the outgoing edges, one traverses every outgoing edge of u with probability of p_{uv} , then the result is equivalent to running a BFS on a reversed instance graph.

Therefore, one approach towards accelerating random RR set generation is to employ parallel algorithms previously proposed for BFS on GPU [22], [23], [24], [25], [26]. Such methods parallelize the procedure of generating one random RR set on GPU.

Most previous solutions on parallelizing BFS on GPU are level-synchronous, that is each level can be processed in parallel, but consecutive levels must be processed sequentially. These methods often maintain a node frontier queue, which is produced by processing the previous level, and is used to produce the node frontier for the next level. In level-synchronous methods, parallelization is usually implemented among the nodes in the current frontier queue or their outgoing edges, therefore, if the size of current frontier is relatively small, then not much gain can be attained from parallelization. Even the overhead of synchronization between consecutive levels can exceed any gain achieved from parallelization. Unfortunately, the problem of small frontier is not rare. Under the LT model, each node has at most one active outgoing edge so the maximum number of nodes in

the frontier does not exceed 1. Even under the IC model, where nodes may have more than one active edge, low values of influence probabilities in real data cause instance graphs to be usually much sparser than G . Therefore, the average number of active edges per node is low and the frontier cannot grow very much.

Liu et al. [27] exploited the similarity between frontiers of BFS traversals started from different nodes and proposed an algorithm to run multiple concurrent BFSs on the same GPU. This algorithm still requires relatively large frontiers to achieve performance gains and is also heavily reliant on the assumption of high resemblance between frontiers, which may not be the case for generating random RR sets.

Another important issue with using previous parallel BFS algorithms is producing redundant nodes in the frontier queue. Since all nodes in the current frontier queue are processed in parallel, a node which is adjacent to more than one node in the current frontier might be placed in the next level's frontier more than once. In standard BFS, this issue may degrade speed, but does not affect the correctness of the algorithm. However, edge traversal in random RR set generation is randomized, and when a node is placed more than once in the frontier, its outgoing edges are processed multiple times, and this issue violates the correctness of RR set generation. For example, if node u is placed in the frontier queue twice, each one of its outgoing edges $e = (u, v)$ are also processed twice, which accordingly increases influence probability from p_{uv} to $1 - (1 - p_{uv})^2$.

3.2 Proposed Parallel Method for RR Set Sampling

The above two approaches are actually located at two extreme ends of the spectrum. One launches many random RR set generation tasks but executes each one of them sequentially, and the other generates a single random RR set at a time and strives to parallelize that single task using all the GPU resources. Our proposed method is located somewhere between these two extremes.

Overview:

We run many random RR set generations in parallel, and also, parallelize the execution of every random RR set generation to some extent. In specific, we judiciously assign the task of generating every random RR set to one CUDA block. See Algorithm 4. Every block is associated with a fixed-size frontier queue in the shared memory which is denoted by Q_{shr} , a *Visited* array of length n to keep account of visited nodes during BFS, and a custom-designed data structure named RR_{tmp} which is used to temporarily hold the generated RR set. Both *Visited* and RR_{tmp} are located in GPU global memory.

The number of RR sets to which a particular node belongs, is an estimator of that node's influence spread. Hence, we also need to maintain the number of occurrences of every node in all the generated RR sets. To do so, we employ array *Occur* of length n , whose elements are initialized to zero.

Data Structure RR_{tmp} :

The number of nodes in an RR set may vary from one to all the nodes. Therefore, RR_{tmp} should be capable of storing an RR set as large as the set V . If RR_{tmp} is implemented

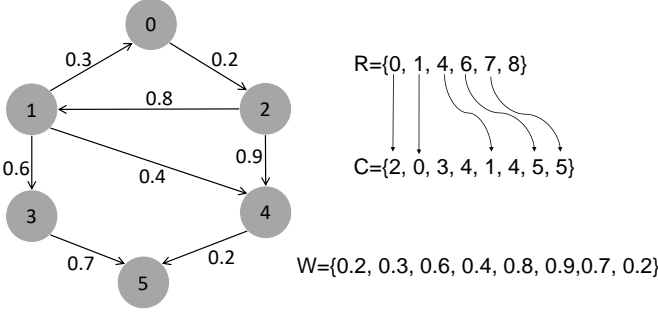


Fig. 1. Example: a graph and its corresponding CSR representation.

as an array of length n , since every block is associated with a RR_{tmp} , the total number of blocks that can be executed in parallel would be restricted by the amount of memory required to store all these large arrays. If RR_{tmp} is implemented as a linked list, whose memory footprint can grow dynamically, the overhead of memory management would be too large. To tackle this issue, we devise a data structure that is similar to a linked list. However, the granularity for memory management is set larger than a single node. In specific, each element in the linked list is composed of a pointer to the next element and a fixed-length array to store some of the nodes.

Graph Representation:

We represent graph G in the compressed sparse row (CSR) format. As illustrated in Fig. 1, the CSR representation consists of two arrays, namely, the column indices array C , and the row offsets array R . For a graph G with n nodes and m edges, array C of size m is created by concatenating adjacency lists of all the nodes in G . Array R has $n + 1$ elements, where element $R[i]$ denotes the location of the adjacency list of node i in array C . One can find all outgoing neighbors of a particular node i , by reading all elements in C indexed from $R[i]$ to $R[i + 1]$. In addition, array W of size m contains influence probability p_{uv} for every edge $e = (u, v)$. Note that in our CSR representation, all the nodes and edges are kept in the same ordering as G , i.e., we do not perform any sorting or pre-processing on the nodes or edges of the input graph G .

Algorithm Details:

Algorithm 4 shows our parallel algorithm for random RR set generation under IC diffusion model. The input graph is represented by R , C and W arrays. Parameter θ is the number of required random RR sets to be generated.

The algorithm works as the following. Every thread within a block is distinguished by an index denoted as tx , which ranges from 0 to $N_{th} - 1$. First, thread zero ($tx = 0$) performs the required initializations, randomly selects a node from V as the source node for BFS, and inserts this node at the front of Q_{shr} (lines 2 – 6). Next, all N_{th} threads start a parallel randomized BFS from the randomly selected node. In this parallel BFS, nodes are processed sequentially and parallelization is realized in evaluation of adjacent edges to the current node. The BFS continues as long as the shared queue Q_{shr} is not empty (line 8).

Algorithm 4 Parallel kernel for random RR set generation (see Section 3.2).

Input: R, C, W, θ

Output: $Occur, RR_{tmp}$

of blocks: θ

of threads / block: N_{th}

```

1: if  $tx == 0$  then
2:    $RR_{tmp}.init()$ 
3:    $Q_{shr}.init()$ 
4:    $Q_{res}.init()$  // Section 3.3
5:    $u = randSelect(V)$ 
6:    $Q_{shr}.enqueue(u)$ 
7: end if
8: while  $!Q_{shr}.empty()$  do
9:    $u = Q_{shr}.front()$ 
10:  if  $tx == 0$  then
11:     $RR_{tmp}.insert(u)$ 
12:     $Q_{shr}.dequeue()$ 
13:     $atomicAdd(Occur[u], 1)$ 
14:  end if
15:   $s = R[u], e = R[u + 1]$ 
16:  for  $(i = tx; i < e - s; i = i + N_{th})$  do
17:     $ofloadQueue(Q_{shr}, Q_{res})$  // Section 3.3
18:     $v = C[s + i], p_{uv} = W[s + i], p = U(0, 1)$ 
19:    if  $p < p_{uv} \ \& \ Visited[v] == false$  then
20:       $Visited[v] = true$ 
21:       $Q_{shr}.atomic_enqueue(v)$ 
22:    end if
23:  end for
24:   $reloadQueue(Q_{shr}, Q_{res})$  // Section 3.3
25: end while

```

If Q_{shr} is not empty, all threads extract the node at the front of Q_{shr} (line 9). Next, thread zero ($tx = 0$) inserts the extracted node to RR_{tmp} , removes it from Q_{shr} , and increments its corresponding element in array $Occur$ (lines 10 – 14). Then, all threads within the block find the range of the extracted node's out-neighbors in array C (line 15). Next, they collaboratively read the out-neighbors of the current node from C and their corresponding influence propagation probabilities from W (line 18). While processing an edge, every thread produces a random number from the uniform distribution $U(0, 1)$, and compares the generated random number with influence probability of that edge, and based on this comparison, it decides whether to traverse that edge or not. When a thread decides to traverse a particular edge, it checks the visited flag of the destination node of that edge, and if the node has not been visited already, it is added to the frontier queue (lines 19 – 22). Since threads within a block are executed in parallel, more than one thread may decide to add a node to Q_{shr} . Therefore adding a node to Q_{shr} should be protected by atomic operations (line 21). Details of $ofloadQueue()$ in line 17 and $reloadQueue()$ in line 24 are discussed in Section 3.3.

3.3 Avoiding Overflow of the Frontier Queue

Shared memory is one of the most limited resources in GPU. In the proposed parallel algorithm, every block uses shared memory to store its own fixed-size frontier queue.

Algorithm 5 *offloadQueue* function

```

1: function OFFLOADQUEUE( $Q_{shr}, Q_{res}$ )
2:   if  $Q_{shr}.size() > \tau_q$  then
3:     if  $tx == 0$  then
4:        $ptr = Q_{res}.alloc()$ 
5:     end if
6:      $ptr[tx] = Q_{shr}.deque\_block(tx)$ 
7:   end if
8: end function

```

Algorithm 6 *reloadQueue* function

```

1: function RELOADQUEUE( $Q_{shr}, Q_{res}$ )
2:   if  $Q_{shr}.empty() \& \& Q_{res}.empty()$  then
3:     if  $tx == 0$  then
4:        $ptr = Q_{res}.pop()$ 
5:     end if
6:      $Q_{shr}.enqueue\_block(ptr[tx], tx)$ 
7:   end if
8: end function

```

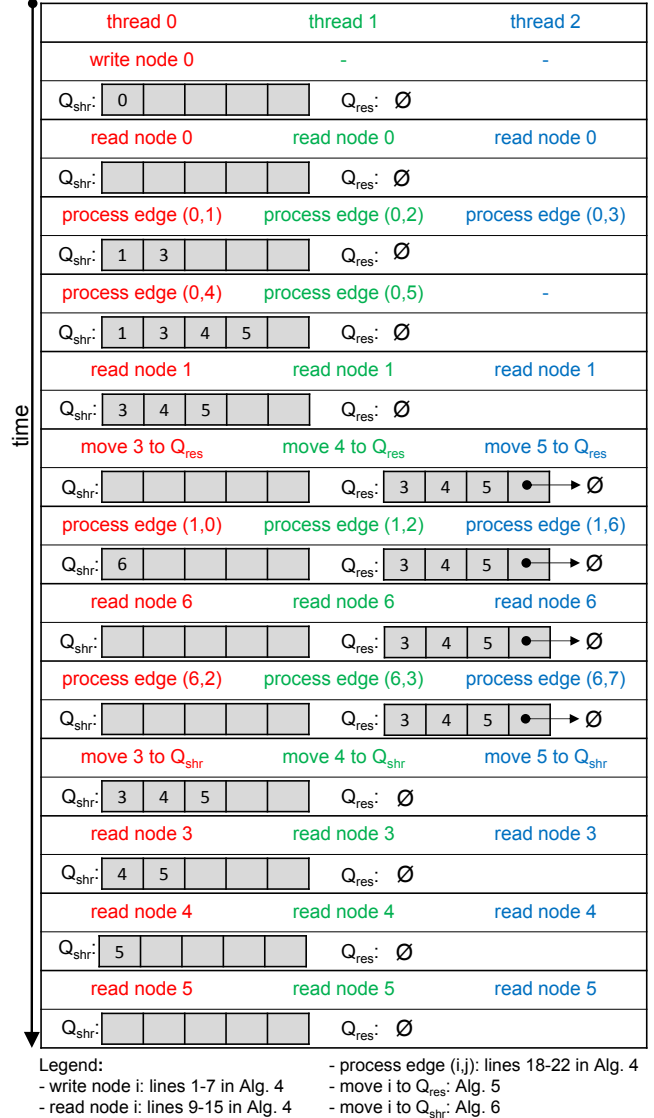
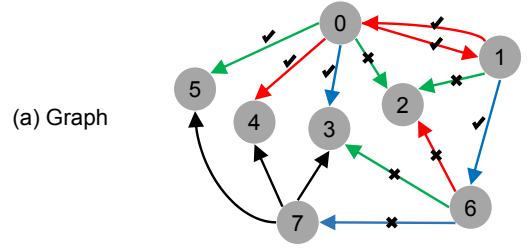
If we allocate small queues, the actual frontier may grow larger and cause the queue to overflow, in which case, the produced RR set is no longer valid. In order to guarantee that no queue overflow occurs, we could increase the queue size to the total number of nodes. However, by doing this, we are no longer able to maintain the queue in GPU shared memory. Moving the queue to GPU global memory incurs long memory access latencies. To resolve this issue, we propose the following solution. We define a threshold τ_q as

$$\tau_q = |Q_{shr}| - N_{th}, \quad (4)$$

where $|Q_{shr}|$ is queue capacity (the maximum number of nodes that every queue may hold), and N_{th} is the total number of threads within a block. When the number of nodes currently stored in the queue exceeds τ_q , there is a chance for the queue to overflow. This is because each one of N_{th} threads within the block processes one edge, and therefore, has a chance to add one new node to the queue. In the worst case, when all N_{th} threads add a node to the queue, overflow occurs.

To resolve this issue, we associate a reservoir queue, to every block, which is denoted by Q_{res} and is actually implemented as a stack whose elements are arrays of length N_{th} . The reservoir queue is stored in GPU global memory and its size may grow dynamically, hence, it does not have shared queue's limitations. Our approach to avoid possible overflows is the following. As shown in line 17 in Algorithm 4, *offloadQueue*() function is executed before all threads process their incident edges. As shown in Algorithm 5, this function checks the condition $Q_{shr}.size() > \tau_q$. If the condition is satisfied, thread zero allocates the required memory to expand the reservoir queue. Then all threads collaboratively move N_{th} elements from the shared queue to the newly allocated space in reservoir queue. This reduces the number of nodes in the shared queue and prevents possible overflow.

The elements of Q_{shr} which have been moved to Q_{res} , need to be returned back to Q_{shr} when it has enough empty space. This procedure is implemented in *reloadQueue*()



(b) Execution Flow

Fig. 2. (a) An example graph. (b) Execution flow of a random RR set generation starting from node 0 within a small block with three threads. Details are discussed in Section 3.4.

function, which is shown in Algorithm 6. In this function, threads check if Q_{shr} is empty and also if there are some nodes in the Q_{res} that can be brought back to Q_{shr} (line 2). If this condition is satisfied, threads collaboratively move N_{th} nodes from Q_{res} to Q_{shr} (line 6).

3.4 An Illustrative Example

Fig. 2 illustrates the execution flow of a random RR set generation a simple graph by using one small CUDA block with $N_{th} = 3$ threads. Since outgoing edges are processed

via parallel threads, edges are marked with different colors according to their corresponding threads. Black edges are not processed throughout this example, because their source node is not visited and thus is not placed in the queue. Check marks and cross marks on the edges represent whether the corresponding edge is traversed or not.

The execution starts by thread zero which places node 0 into Q_{shr} . Next, node 0 is extracted by all threads and its outgoing edges are processed. Since node 0 has more than $N_{th} = 3$ outgoing edges, processing these edges are performed in two consecutive steps and newly visited nodes are put in Q_{shr} . Then, node 1 is extracted from Q_{shr} , but threads find that $N_q = 3 > \tau_q = 2$, so N_{th} nodes are moved from Q_{shr} to Q_{res} . Next, outgoing edges of node 1 are processed, and recently visited node 6 is added to Q_{shr} . In the next step, node 6 is extracted from Q_{shr} and its outgoing edges are processed. Afterwards, threads find that Q_{shr} is empty and thus bring back N_{th} nodes from Q_{res} to Q_{shr} . The rest of the procedure is straightforward. Nodes are removed from the queue one by one until both Q_{shr} and Q_{res} become empty.

3.5 Optimizing Memory Usage

In most cases, size of the generated RR set is very small, and therefore, RR_{tmp} data structure has only few elements and the allocated array inside the last element of this data structure is underutilized. This under-utilization of GPU global memory should be avoided since the number of RR sets to be generated is large.

To this end, Algorithm 4 is modified as shown in Algorithm 7. Right after producing an RR set, it is copied from RR_{tmp} to a continuous chunk of memory called RR . This data structure is basically formed by concatenation of all the generated RR sets.

In addition, the total number of concurrent blocks is reduced from θ (the number of RR sets to be generated) to a constant number N_b . This is done because every block requires to store intermediate data (i.e., Q_{res} and $Visited$) in GPU global memory.

In Algorithm 7, N_{RR} and $tail_{RR}$ are scalar variables which lie in GPU global memory and keep track of the number of generated random RR sets so far, and the sum of their sizes, respectively. Once a random RR set is generated (line 2), the location where it should be copied to in array RR is determined and stored in $Offsets_{RR}$ (lines 4 – 5). This is required so that the boundaries between consecutive random RR sets in array RR can be distinguished later. In addition, N_{RR} is incremented by 1, and $tail_{RR}$ is incremented by the size of the generated RR set (lines 6 – 7). Finally, all threads within the block collaboratively copy the generated RR set from RR_{tmp} to the specified location in array RR (lines 9 – 11). A block terminates its execution when the number of generated RR sets has reached the number of required RR sets (line 12).

Note that since N_{RR} and $tail_{RR}$ are accessible by all concurrent blocks, lines 4 – 7 should be protected from concurrent execution using mutex and atomicCAS in CUDA API. For brevity, this is not shown in Algorithm 7.

Without the optimization presented in this section, the required data would not fit into GPU global memory. For example, storing one $Visited$ array for a graph with 4 million

Algorithm 7 Memory-optimized parallel kernel for random RR set generation (see Section 3.5).

Input: R, C, W, θ

Output: $Occur, RR$

of blocks: N_b

of threads / block: N_{th}

```

1: repeat
2:   Generate one random RR set as in Algorithm 4
3:   if  $tx == 0$  then
4:      $offset = tail_{RR}$ 
5:      $Offsets_{RR}[N_{RR}] = offset$ 
6:      $N_{RR} = N_{RR} + 1$ 
7:      $tail_{RR} = tail_{RR} + RR_{tmp}.size()$ 
8:   end if
9:   for ( $i = tx$ ;  $i < RR_{tmp}.size()$ ;  $i = i + N_{th}$ ) do
10:     $RR[offset + i] = RR_{tmp}[i]$ 
11:   end for
12: until  $N_{RR} \leq \theta$ 

```

nodes requires about 488 kB of GPU global memory, hence, if we were to launch θ blocks instead of N_b blocks, launching $\theta = 1$ million blocks would require 465 GB of GPU global memory only to store all the $Visited$ arrays. This is about 10 to 60 times larger than the amount of memory available on even high-end GPUs today.

3.6 Modifications under the LT Model

Our proposed parallel algorithm for random RR set sampling can be modified to support LT diffusion model as well. Under this model, every node has at most one active incoming edge, which is selected randomly according to the edge weights. First, thread zero samples a random number from $U(0, 1)$. Then all threads within the block run a parallel scan algorithm [28] on the edge weights, and instead of comparing the generated random number with edge weights, they compare it with two consecutive numbers that resulted from the parallel scan. The first thread that finds the generated random number between two consecutive outputs of scan, marks its edge as active and broadcasts an early termination signal to all other threads within the block.

In addition, since every node visits at most one other node during random BFS, the size of the frontier queue never exceeds one, and therefore, the fixed-size shared frontier queue never overflows and the reservoir queue is not required anymore.

3.7 Proposed Parallel Method for Seed Set Generation

The final step is to solve the Maximum Coverage problem on the generated random RR sets, in order to generate the seed set. IMM [8] used the standard greedy algorithm to solve this problem, which is illustrated in lines 6 – 10 of Algorithm 2.

Our proposed solution, however, employs a more efficient approach. As mentioned in Section 3.2, every node is associated with a counter which keeps track of the number of its occurrences across all the generated random RR sets. All such counters are stored in array $Occur$. By running a

Algorithm 8 Maximum Coverage parallel kernel.**Input:** $RR, Occur, u$ **Output:** $Occur, Covered$ # of blocks: N_b # of threads / block: N_{th}

```

1: for ( $i = bx; i < N_{RR}; i = i + N_b$ ) do
2:   if  $Covered[i] == false$  then
3:      $found = false$ 
4:      $offset = Offsets_{RR}[i]$ 
5:      $length = Offsets_{RR}[i + 1] - offset$ 
6:     for ( $j = tx; j < length \& !found; j = j + N_{th}$ ) do
7:       if  $RR[offset + j] == u$  then
8:          $found = true$ 
9:       end if
10:    end for
11:    if  $found == true$  then
12:       $Covered[i] = true$ 
13:      for ( $j = tx; j < length; j = j + N_{th}$ ) do
14:         $atomicAdd(Occur[RR[offset + j]], -1)$ 
15:      end for
16:    end if
17:  end if
18: end for

```

parallel reduction algorithm [29] with max operator on this array, the node with maximum coverage is found.

Once a node is selected and added to the seed set, all RR sets which contain that node must be removed, and also, all counters whose corresponding nodes are present in those RR sets must be decremented. To do this, we associate every RR set with a *Covered* flag which indicates whether or not the RR set is covered by the seed set so far. In order to mark the covered RR sets and update the counters, we employ the parallel kernel shown in Algorithm 8. Here, the generated RR sets are distributed among N_b blocks (line 1). When a block processes an RR set, it first checks that the RR set has not already been covered by any node in the seed set (line 2). Then, all threads within the block collaboratively search for all occurrences of node u , i.e., the newly added node in the seed set (lines 3 – 10). If the RR set contains node u , it is flagged as covered, and all threads within the block collaboratively decrement the counters whose corresponding nodes are present in this RR set (lines 11 – 16).

3.8 Synchronization

To ensure correct functionality, we need to synchronize all threads within a block after lines 7, 9 and 14 in Algorithm 4, line 5 in Algorithm 5, line 5 in Algorithm 6, and lines 2 and 10 in Algorithm 8. For brevity, these are not shown in the pseudo-codes.

4 EXPERIMENTAL EVALUATION

4.1 Setup

The proposed parallel algorithm is implemented in C++ language using CUDA parallel programming framework. We employ CUB library [30] for parallel reduction and

TABLE 1
Benchmark datasets.

Dataset	Type	# of nodes (n)	# of edges (m)
soc-Epinions1	Directed	75,879	508,837
soc-Slashdot0922	Directed	77,360	905,468
higgs-twitter	Directed	456,631	14,855,875
soc-Pokec	Directed	1,632,803	30,622,564
soc-LiveJournal1	Directed	4,847,571	68,993,773
com-Orkut	Undirected	3,072,441	117,185,083

sorting on GPU, and Thrust library [31] to facilitate memory management on GPU.

Benchmark datasets are graphs extracted from real social networks. All the benchmarks are publicly available and can be downloaded from [32]. The main characteristics of these datasets are shown in Table 1.

We compare our proposed algorithm with IMM [8], [33] and SKIM [34]. IMM is the state-of-the-art algorithm which provides theoretical guarantee on the approximation ratio of influence spread, and SKIM is among the best algorithms which does not provide the theoretical guarantee but runs faster than IMM.

To run the experiments, we employed a Linux machine with Intel Xeon CPU operating at 2.50 GHz, and Tesla V100 GPU operating at 1245 MHz. We employ CUDA version 10.2. Since IMM [33] and SKIM [34] are sequential methods, they are executed on a single CPU core. In our proposed solution, the parallel kernels are executed on the GPU, and the rest of the program is executed on a single CPU core.

Although some efforts [35], [36], [37] have been made to learn influence probabilities based on user actions extracted from social networks, most previous works used simple heuristics to assign influence probabilities to the edges. Weighted Cascade (WC) [1] is one of the most commonly used schemes in previous works. In this scheme, the influence probability of edge $e = (u, v)$ is set to $1/d_v^{in}$, where d_v^{in} is the in-degree of node v . By using this scheme, the probability of a node being influenced is heuristically less dependent on the number of incoming edges. Also, WC scheme, in which the sum of incoming edges' probabilities for each node is exactly equal to 1, can be used under the LT model. In our experiments, we use WC scheme to assign influence probabilities to edges, under both IC and LT models.

4.2 Performance Comparison

Table 2 illustrates the runtime of different methods with $k = 50$ and $\epsilon = 0.05$ under the IC model in different datasets. We used the default parameters in the evaluation of SKIM. It is noteworthy to mention that the solution quality, i.e., the influence spread of the resulting seed set, is the same for IMM and the proposed solution, however, the solution quality of SKIM is slightly lower (about 1% to 3% lower).

The runtime of IMM varies from 4.42 seconds to 813.09 seconds, and it increases as graph size grows. SKIM runs faster than IMM. The runtime varies from 0.29 to 36.53 seconds. The proposed solution, however, attains much smaller runtime compared to both IMM and SKIM. Our solution's runtime ranges from 131 milliseconds to 3.689 seconds. Note that the measured runtime values include all

TABLE 2
Runtime of different methods under IC diffusion model.

		soc-Epinions1	soc-Slashdot0922	higgs-twitter	soc-Pokec	soc-LiveJournal1	com-Orkut
Runtime (sec.)	IMM	4.42	12.69	92.94	122.91	251.86	813.09
	SKIM	0.29	0.58	2.49	4.43	7.71	36.53
	Proposed	0.131	0.143	0.802	1.084	2.276	3.689
Speedup ratio over IMM	SKIM	15.24	21.87	37.33	27.74	32.67	7.82
	Proposed	33.74	88.74	115.89	113.39	110.66	220.41

overheads such as CPU to GPU data transfer latency. The speedup ratio of the proposed method over IMM ranges from $33.74\times$ to $220.41\times$.

4.3 Impact of Parameters k and ϵ

The number of required random RR sets to guarantee $(1 - \frac{1}{e} - \epsilon)$ -approximation ratio, which directly affects runtime, is dependent on the values of k and ϵ . Fig. 3 and Fig. 4 compare the runtime of our algorithm against IMM with $\epsilon = 0.1$ and for different values of k . As can be seen, the speedup factor is relatively consistent for different values of k . It can be seen that the runtime of IMM is monotonically increasing, while the runtime of our work sometimes drops when k increases. This is because by increasing the value of k , the amount of influence of the seed set also increases and it might cause the condition in line 7 of Algorithm 3 to be satisfied one iteration earlier. In IMM, calling greedy seed set generation procedure for one fewer iteration does not significantly affect the runtime, because random RR set generation is the dominant contributor to the runtime. While in our work, random RR generation experiences much higher speedup in comparison with greedy seed selection. Therefore, the greedy seed selection procedure calls become dominant in the total runtime, and one fewer iteration to this procedure can decrease the runtime in spite of the increased required number of RR sets.

We also studied the impact of ϵ on runtime. Fig. 5 illustrates the running times for different values of ϵ with $k = 50$. The number of required RR samples (i.e., θ) has an inverse quadratic relation with the value of ϵ . As can be seen, the runtime values follow the same trend, and therefore the amount of speedup is almost preserved for different values of ϵ .

4.4 Scalability

In this section, we evaluate the scalability of our proposed algorithm. Specifically, we measure the runtime of our algorithm against IMM on synthetic graphs with varying densities and show that the speedup increases, as the density of the input graph grows.

In order to generate synthetic graphs, we use Barabasi-Albert model [38], which is an algorithm for generating undirected random scale-free graphs by using preferential attachment mechanism. This algorithm starts with a clique of r_0 nodes, and then, new nodes are added one by one. Every newly added node is randomly connected to r nodes that are already in the graph ($r \leq r_0$). The constant parameter r is the graph density. The probability that the newly added node is connected to node i is determined by the following equation:

$$p_i = \frac{d_i}{\sum_j d_j}, \quad (5)$$

where d_i denotes the current degree of node i , and the sum is over the nodes that already exist in the graph. It has been proven that Barabasi-Albert model generates a graph with a power law degree distribution [39].

We generated various graphs with $n = 10^6$ nodes and different densities ranging from $r = 2$ to $r = 32$, by using Barabasi-Albert algorithm. We measure the runtime of our algorithm and IMM over the generated graphs, with parameters $k = 50$ and $\epsilon = 0.05$. Fig. 6 illustrates the resulting runtimes and speedup. As can be seen, the speedup increases, as r grows. This observation can be attributed to the way by which edges are processed in our algorithm: N_{th} threads within a warp process all outgoing edges of a single node. Therefore, if the number of outgoing edges of a node is less than N_{th} , some threads remain idle and perform no useful computation. When r grows, the average degree also increases, and as a result, fewer threads remain idle and more potential parallelism can be exploited.

4.5 Multi-round Influence Maximization

Although some proposed algorithms for solving the standard influence maximization problem have successfully been used to resolve some real-world problems [40], [41], it is evident that the standard IM problem cannot grasp all aspects of real-world phenomena. Therefore, many researchers have attempted to propose new variations of the standard IM problem, in order to incorporate new details such as time restriction [11], [13], location awareness [42], [43] and topic awareness [44] into the standard IM problem and make it more realistic for real-world situations. Interestingly, most of the variations to the IM problem can be easily solved by making some subtle modifications to RIS-based algorithms. Therefore, our parallel algorithm not only is able to solve the standard IM problem in a very short time but also is capable of solving different variations of it by applying simple modifications. In order to illustrate this, we introduce a specific variation of the IM problem called multi-round influence maximization [7] and show that our algorithm is able to solve this problem.

In the multi-round influence maximization problem (MRIM), influence propagates in multiple rounds, and the goal is to find a seed set for each round in order to maximize the total number of nodes that have been influenced at least once. Sun et al. [7] proposed three different algorithms to solve the MRIM problem, all of which can be implemented efficiently by using reverse influence sampling. We slightly modify our algorithm to parallelize CR-NAIMM algorithm

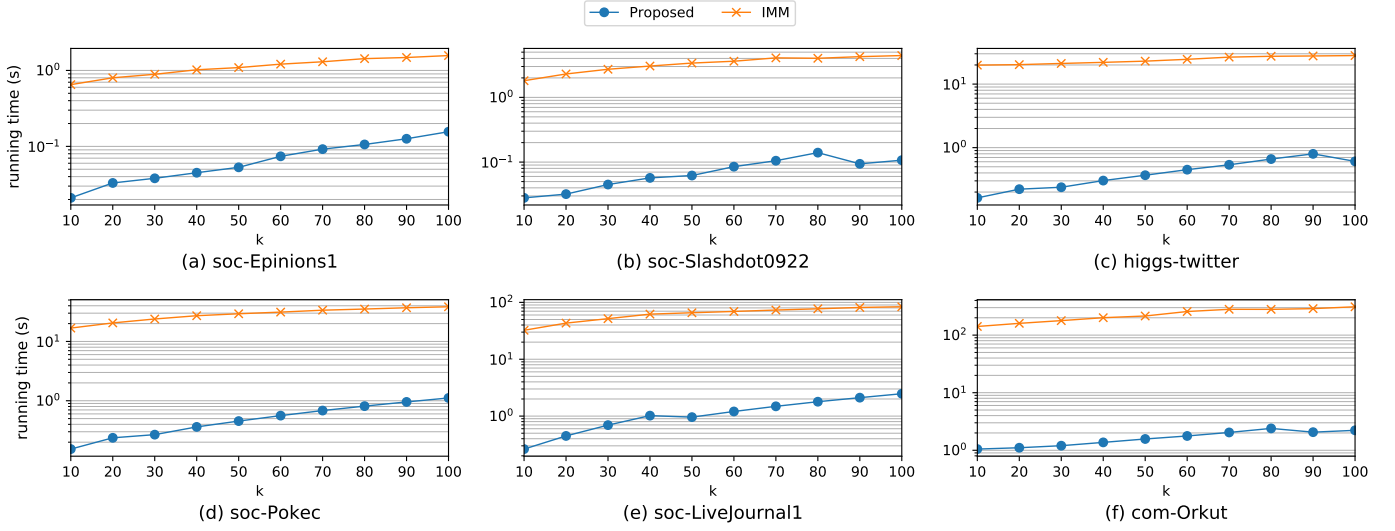


Fig. 3. Runtime of algorithms for different values of k with $\epsilon = 0.1$ under IC model.

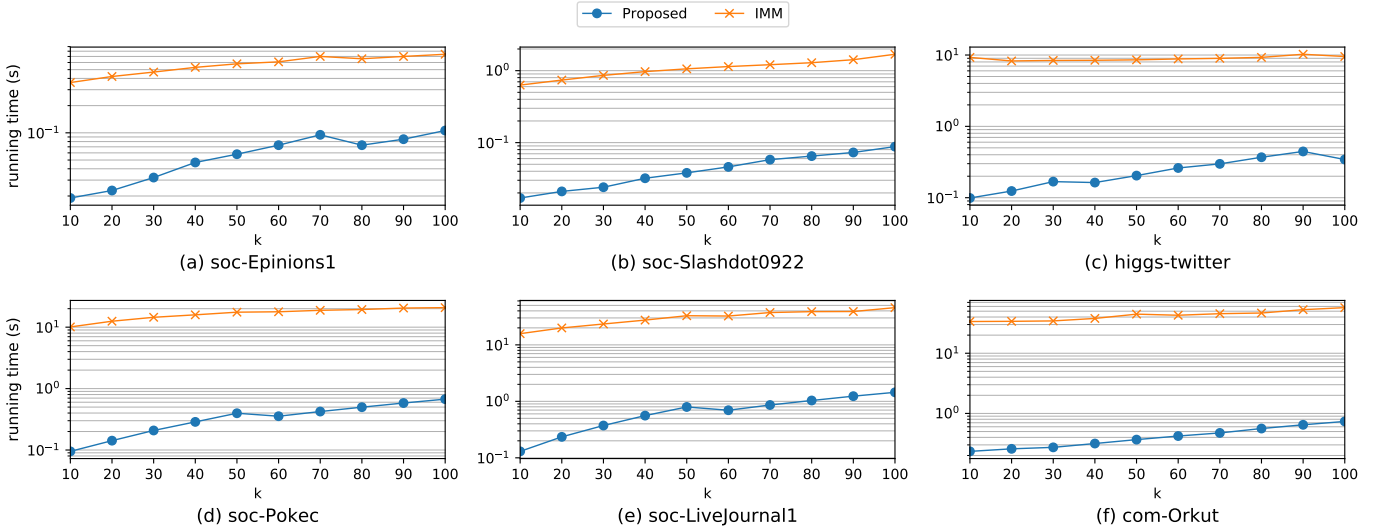


Fig. 4. Runtime of algorithms for different values of k with $\epsilon = 0.1$ under LT model.

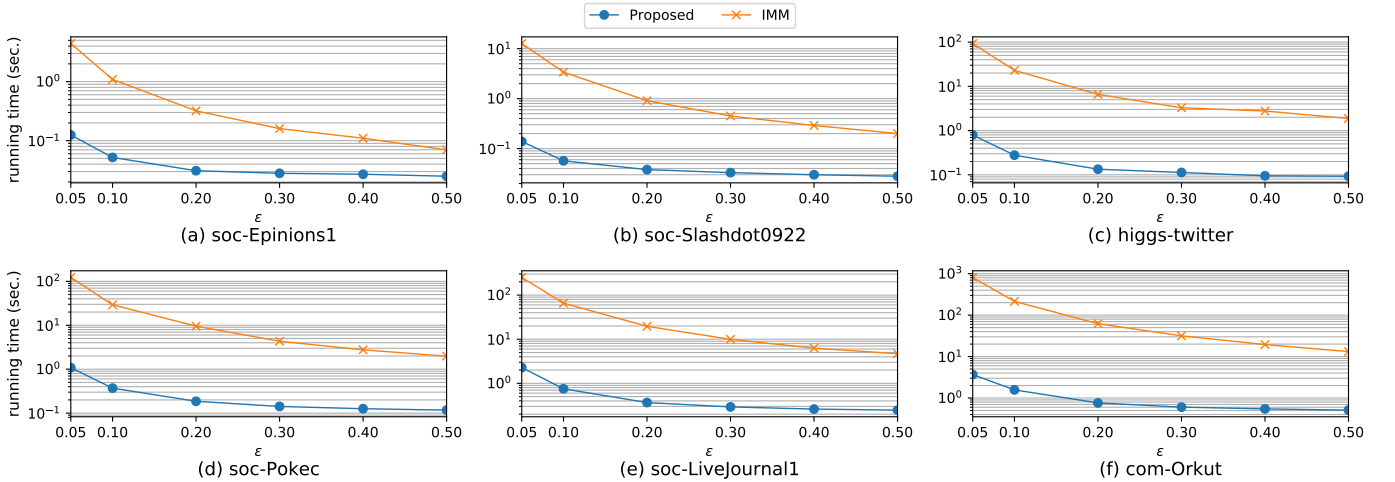


Fig. 5. Runtime of algorithms for different values of ϵ with $k = 50$ under IC model.

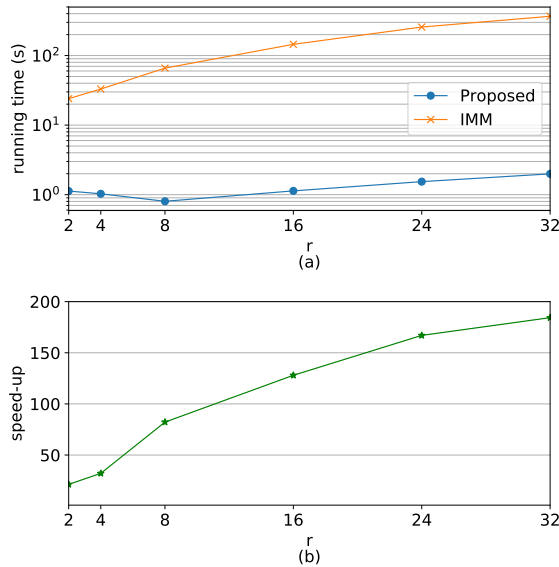


Fig. 6. (a) Runtime of IMM and our proposed solution on random scale-free graphs with different densities. (b) The resulting speedup, i.e., the ratio of the two curves in (a).

TABLE 3
Running time of CR-NAIMM algorithm in seconds.

Dataset	GPU	CPU	Speed-up
soc-Epinions1	0.087	2.4	27.59
soc-Slashdot0922	0.066	8.97	135.91
higgs-twitter	0.74	56	75.68
soc-Pokec	2.055	60	29.13
soc-LiveJournal1	10.755	113	10.51
com-Orkut	5.118	591	115.47

in [7], which is more computationally expensive than the others. Specifically, after selecting a random node, we initiate a random BFS originating from the selected node as many times as the number of rounds. Also, each element in a random RR set is a tuple of node-id and round number. The rest of our algorithm remains almost intact. We performed experiments using real-world datasets. We set the size of the seed set to $k = 10$, the number of rounds to $T = 5$, and $\epsilon = 0.1$. The runtimes of both serial and parallel algorithms on different datasets are shown in Table 3. We achieve a speed-up of up to $136\times$ and an average of $65.72\times$ on six datasets.

5 CONCLUSION

With larger role that nowadays social networks are playing in our lives, they have attracted a lot of attention to be used as an effective platform for viral marketing campaigns. This has caused IM problem to emerge as an algorithmic method to find top influential individuals in a social network. Despite numerous works that tried to enhance the scalability by proposing new algorithms, there is still a lack of scalability, especially on large graphs. In this paper, we proposed an efficient parallel implementation of IMM algorithm on GPU. Extensive experiments on real social network graphs demonstrated that our algorithm significantly reduces the runtime of IMM. Moreover, we show that our algorithm

is able to solve other variants of the IM problem, only by applying minor modifications.

REFERENCES

- [1] D. Kempe, J. Kleinberg, and É. Tardos, "Maximizing the spread of influence through a social network," in *Proceedings of the ninth ACM SIGKDD international conference on Knowledge discovery and data mining*. ACM, 2003, pp. 137–146.
- [2] W. Chen, Y. Yuan, and L. Zhang, "Scalable influence maximization in social networks under the linear threshold model," in *2010 IEEE international conference on data mining*. IEEE, 2010, pp. 88–97.
- [3] W. Chen, C. Wang, and Y. Wang, "Scalable influence maximization for prevalent viral marketing in large-scale social networks," in *Proceedings of the 16th ACM SIGKDD international conference on Knowledge discovery and data mining*. ACM, 2010, pp. 1029–1038.
- [4] J. Leskovec, A. Krause, C. Guestrin, C. Faloutsos, J. VanBriesen, and N. Glance, "Cost-effective outbreak detection in networks," in *Proceedings of the 13th ACM SIGKDD international conference on Knowledge discovery and data mining*, 2007, pp. 420–429.
- [5] A. Goyal, W. Lu, and L. V. Lakshmanan, "Celf++ optimizing the greedy algorithm for influence maximization in social networks," in *Proceedings of the 20th international conference companion on World wide web*, 2011, pp. 47–48.
- [6] X. He and D. Kempe, "Stability of influence maximization," in *Proceedings of the 20th ACM SIGKDD international conference on Knowledge discovery and data mining*, 2014, pp. 1256–1265.
- [7] L. Sun, W. Huang, P. S. Yu, and W. Chen, "Multi-round influence maximization," in *Proceedings of the 24th ACM SIGKDD International Conference on Knowledge Discovery & Data Mining*, 2018, pp. 2249–2258.
- [8] Y. Tang, Y. Shi, and X. Xiao, "Influence maximization in near-linear time: A martingale approach," in *Proceedings of the 2015 ACM SIGMOD International Conference on Management of Data*, 2015, pp. 1539–1554.
- [9] S. Wen, M. S. Haghighi, C. Chen, Y. Xiang, W. Zhou, and W. Jia, "A sword with two edges: Propagation studies on both positive and negative information in online social networks," *IEEE Transactions on Computers*, vol. 64, no. 3, pp. 640–653, 2014.
- [10] Y. Li, W. Chen, Y. Wang, and Z.-L. Zhang, "Influence diffusion dynamics and influence maximization in social networks with friend and foe relationships," in *Proceedings of the sixth ACM international conference on Web search and data mining*, 2013, pp. 657–666.
- [11] W. Chen, W. Lu, and N. Zhang, "Time-critical influence maximization in social networks with time-delayed diffusion process," in *Twenty-Sixth AAAI Conference on Artificial Intelligence*, 2012.
- [12] J. Kim, W. Lee, and H. Yu, "Ct-ic: Continuously activated and time-restricted independent cascade model for viral marketing," *Knowledge-Based Systems*, vol. 62, pp. 57–68, 2014.
- [13] B. Liu, G. Cong, D. Xu, and Y. Zeng, "Time constrained influence maximization in social networks," in *2012 IEEE 12th international conference on data mining*. IEEE, 2012, pp. 439–448.
- [14] M. G. Rodriguez, D. Balduzzi, and B. Schölkopf, "Uncovering the temporal dynamics of diffusion networks," *arXiv preprint arXiv:1105.0697*, 2011.
- [15] M. Xie, Q. Yang, Q. Wang, G. Cong, and G. De Melo, "Dynadiffuse: A dynamic diffusion model for continuous time constrained influence maximization," in *Twenty-Ninth AAAI Conference on Artificial Intelligence*, 2015.
- [16] W. Chen, L. V. Lakshmanan, and C. Castillo, "Information and influence propagation in social networks," *Synthesis Lectures on Data Management*, vol. 5, no. 4, pp. 1–177, 2013.
- [17] C. Borgs, M. Brautbar, J. Chayes, and B. Lucier, "Maximizing social influence in nearly optimal time," in *Proceedings of the twenty-fifth annual ACM-SIAM symposium on Discrete algorithms*. SIAM, 2014, pp. 946–957.
- [18] Y. Tang, X. Xiao, and Y. Shi, "Influence maximization: Near-optimal time complexity meets practical efficiency," in *Proceedings of the 2014 ACM SIGMOD international conference on Management of data*, 2014, pp. 75–86.
- [19] H. T. Nguyen, M. T. Thai, and T. N. Dinh, "Stop-and-stare: Optimal sampling algorithms for viral marketing in billion-scale networks," in *Proceedings of the 2016 International Conference on Management of Data*, 2016, pp. 695–710.
- [20] D. Williams, *Probability with martingales*. Cambridge university press, 1991.

- [21] K. Huang, S. Wang, G. Bevilacqua, X. Xiao, and L. V. Lakshmanan, "Revisiting the stop-and-stare algorithms for influence maximization," *Proceedings of the VLDB Endowment*, vol. 10, no. 9, pp. 913–924, 2017.
- [22] L. Luo, M. Wong, and W.-m. Hwu, "An effective gpu implementation of breadth-first search," in *Design Automation Conference*. IEEE, 2010, pp. 52–55.
- [23] F. Busato and N. Bombieri, "Bfs-4k: an efficient implementation of bfs for kepler gpu architectures," *IEEE Transactions on Parallel and Distributed Systems*, vol. 26, no. 7, pp. 1826–1838, 2014.
- [24] H. Liu and H. H. Huang, "Enterprise: breadth-first graph traversal on gpus," in *Proceedings of the International Conference for High Performance Computing, Networking, Storage and Analysis*, 2015, pp. 1–12.
- [25] D. Merrill, M. Garland, and A. Grimshaw, "Scalable gpu graph traversal," *Acm Sigplan Notices*, vol. 47, no. 8, pp. 117–128, 2012.
- [26] S. Hong, T. Oguntebi, and K. Olukotun, "Efficient parallel graph exploration on multi-core cpu and gpu," in *2011 International Conference on Parallel Architectures and Compilation Techniques*. IEEE, 2011, pp. 78–88.
- [27] H. Liu, H. H. Huang, and Y. Hu, "ibfs: Concurrent breadth-first search on gpus," in *Proceedings of the 2016 International Conference on Management of Data*, 2016, pp. 403–416.
- [28] M. Harris, S. Sengupta, and J. D. Owens, "Parallel prefix sum (scan) with cuda," *GPU gems*, vol. 3, no. 39, pp. 851–876, 2007.
- [29] M. Harris *et al.*, "Optimizing parallel reduction in cuda," *Nvidia developer technology*, vol. 2, no. 4, p. 70, 2007.
- [30] Duane Merrill, "CUB." [Online]. Available: <https://nvlabs.github.io/cub/>
- [31] N. Bell and J. Hoberock, "Thrust: A productivity-oriented library for cuda," in *GPU computing gems Jade edition*. Elsevier, 2012, pp. 359–371.
- [32] J. Leskovec and A. Krevl, "SNAP Datasets: Stanford large network dataset collection," <http://snap.stanford.edu/data>, Jun. 2014.
- [33] [Online]. Available: <https://sourceforge.net/projects/im-imm/>
- [34] E. Cohen, D. Delling, T. Pajor, and R. F. Werneck, "Sketch-based influence maximization and computation: Scaling up with guarantees," in *Proceedings of the 23rd ACM International Conference on Conference on Information and Knowledge Management*, 2014, pp. 629–638.
- [35] K. Saito, R. Nakano, and M. Kimura, "Prediction of information diffusion probabilities for independent cascade model," in *International conference on knowledge-based and intelligent information and engineering systems*. Springer, 2008, pp. 67–75.
- [36] A. Goyal, F. Bonchi, and L. V. Lakshmanan, "Learning influence probabilities in social networks," in *Proceedings of the third ACM international conference on Web search and data mining*, 2010, pp. 241–250.
- [37] K. Kutikov, A. Bifet, F. Bonchi, and A. Gionis, "Strip: stream learning of influence probabilities," in *Proceedings of the 19th ACM SIGKDD international conference on Knowledge discovery and data mining*, 2013, pp. 275–283.
- [38] A.-L. Barabási and R. Albert, "Emergence of scaling in random networks," *science*, vol. 286, no. 5439, pp. 509–512, 1999.
- [39] A.-L. Barabási, R. Albert, and H. Jeong, "Mean-field theory for scale-free random networks," *Physica A: Statistical Mechanics and its Applications*, vol. 272, no. 1-2, pp. 173–187, 1999.
- [40] A. Yadav, H. Chan, A. X. Jiang, H. Xu, E. Rice, and M. Tambe, "Using social networks to aid homeless shelters: Dynamic influence maximization under uncertainty," in *AAMAS*, vol. 16, 2016, pp. 740–748.
- [41] D. L. Gibbs and I. Shmulevich, "Solving the influence maximization problem reveals regulatory organization of the yeast cell cycle," *PLoS computational biology*, vol. 13, no. 6, p. e1005591, 2017.
- [42] C. Zhang, L. Shou, K. Chen, G. Chen, and Y. Bei, "Evaluating geo-social influence in location-based social networks," in *Proceedings of the 21st ACM international conference on Information and knowledge management*, 2012, pp. 1442–1451.
- [43] G. Li, S. Chen, J. Feng, K.-l. Tan, and W.-s. Li, "Efficient location-aware influence maximization," in *Proceedings of the 2014 ACM SIGMOD international conference on Management of data*, 2014, pp. 87–98.
- [44] W. Chen, T. Lin, and C. Yang, "Real-time topic-aware influence maximization using preprocessing," *Computational social networks*, vol. 3, no. 1, p. 8, 2016.